# Supporting Information

## Olzmann et al. 10.1073/pnas.1213738110

### SI Methods

**Plasmids and Antibodies.** The S-tagged and myc-tagged UBXD8, UBAC2, gp78, Hrd1, Derlin-1, AUP1, and ERLIN-2 expression constructs have been described previously (1, 2). The C-terminally S-tagged UBXD8(ΔUBX) construct was generated by PCR amplification of UBXD8(ΔUBX) (amino acids 1–357) and ligation into the XbaI/KpnI sites of the pcDNA3.1–S-tag construct (2). Additional plasmids used include adipose triglyceride lipase (ATGL)-GFP (a kind gift from Juan Bonifacino, National Institutes of Health, Bethesda, MD), PLIN1-GFP and PLIN2-GFP (kind gifts from Raphael Valdivia, Duke University, Durham, NC), and ATGL(S47A)-YFPc and YFPn-CGI-58 (kind gifts from David Savage, University of Cambridge, Cambridge, UK). YFPn-UBXD8 was cloned by PCR amplification of full-length UBXD8 (amino acids 1–445) and ligation into the KpnI/XbaI sites of the pcDNA3.1-YFPn construct (3).

The following antibodies were used: anti–S-tag [rabbit polyclonal, generated previously (2)], anti-myc (9E10; Sigma Aldrich), anti-KDEL (Stressgen), anti-ATGL (Cell Signaling), anti-p97/VCP (Novus Biologicals), anti–CGI-58 (Proteintech Group Inc.), anti–Derlin-2 (a kind gift from Yihong Ye, National Institutes of Health, Bethesda, MD), anti-UBAC2 (a kind gift from Peter Espenshade, Johns Hopkins, Baltimore, MD), anti-PLIN3 (a kind gift from Susan Pfeffer, Stanford University, Stanford, CA), and anti-AUP1 and anti-UBXD8 (kind gifts from Hidde Ploegh, Whitehead Institute for Biomedical Research, Cambridge, MA). HRP-conjugated and Alexa Fluor-conjugated secondary antibodies were purchased from Amersham and Invitrogen, respectively.

**Virus Production and Generation of Stably Transduced Cell Lines.** The pSUPER-RETRO-PURO retroviral vector (Oligoengine) expressing UBAC2-targeting shRNA (GCCATTACATTAGCATGTATT) was generated by ligation of annealed oligos into the BglII/HindIII sites. Empty pSUPER-RETRO was used as the negative control for experiments. Retrovirus was generated by cotransfection of the retroviral plasmid with pCG-GagPol and pVSV-G using FuGENE6 (Roche). Tissue culture supernatant containing infectious virus particles was added to HEK293 or HeLa cells three times over the course of 72 h, and stably transduced cells were selected by incubation with 1 μg/mL puromycin.

**Cell Culture and Transfection.** HEK293, HeLa, and 3T3-L1 cell lines were maintained at 37 °C in DMEM (Mediatech) supplemented with 10% animal serum complex (Gemini Bio-Products) using standard cell culture techniques. The clonal HEK293 cells expressing UBXD8-S, UBAC2-S, GFPu, and TCRα-GFP were described previously (1, 4, 5). The U2OS cells expressing inducible VCP(WT) and VCP(EQ) were kind gifts from Conrad Weihl and Phyllis Hanson (Washington University, Saint Louis, MO). The WT and ATGL$^{-/-}$ MEFs were a kind gift from Rudolph Zechner (University of Graz, Graz, Austria). MEFs, U2OS, and Huh7 cell lines were maintained at 37 °C in DMEM (Mediatech) supplemented with 10% FBS. Cells were transfected using FuGENE6 (Roche) according to the manufacturer's instructions. In brief, DNA:FuGENE6 complexes were prepared in a 1:3 ratio in OPTI-MEM. After a 20-min incubation, complexes were added directly to cells in complete growth medium.

**Differentiation of 3T3-L1 Adipocytes.** The 3T3-L1 preadipocytes were grown to 2 d postconfluency (day 0). The cells were then incubated for 2 d with growth medium supplemented with 115 μg/mL isobutylmethylxanthine, 1 μg/mL insulin, and 1 μM dexamethasone; for 2 d with growth media supplemented with 1 μg/mL insulin; and for 4 d with standard growth medium. Full differentiation was achieved by day 8, and cells were fixed or lysed for experiments.

**Immunodepletion of Protein Complexes.** Lipid droplet (LD)-enriched fractions solubilized in a lysis buffer containing 20 mM Tris·HCl (pH 7.4), 150 mM NaCl, and 1% Triton X-100 supplemented with Complete Protease Inhibitor Mixture (Roche) were incubated with anti-UBXD8 or anti–CGI-58 antibodies, and complexes were isolated by incubation with protein G agarose (Millipore). The flow-through from these incubations was analyzed by SDS/PAGE and immunoblot analysis.

**LD Synthesis and Turnover.** As shown in Fig. 3*A*, HeLa cells were incubated in growth medium containing 10 μM triacsin C for 16 h to deplete cells of any basal LDs. Cells were then washed with growth media, and 200 μM oleate was added for 3 h to induce the simultaneous generation of LDs. Cells accumulate LDs beyond this time point if the oleate treatment is continued, indicating that a 3-h oleate treatment does not saturate cellular LD biosynthetic pathways. For evaluation of LD turnover, cells were washed with growth medium and incubated for an additional 3, 6, or 12 h in growth medium containing 10 μM triacsin C.

**Fluorescence Microscopy and Quantification.** Cells grown on poly-L-lysine–coated coverslips were incubated in the presence or absence of 200 μM oleate for 16–24 h. Cells were then washed with PBS, fixed for 15 min in PBS containing 4% (wt/vol) paraformaldehyde, and washed again with PBS. The fixed cells were permeabilized by incubation with staining buffer [PBS and 1% (wt/vol) bovine serum albumin] containing 0.1% Triton X-100 for 30 min at room temperature. Cells were subsequently incubated with primary antibodies in staining buffer for 2 h, washed with staining buffer, incubated with Alexa Fluor-conjugated secondary antibodies (Invitrogen) for 1 h, washed with staining buffer, and subsequently mounted in mounting medium (Electron Microscopy Sciences). For staining of nuclei, DAPI (Invitrogen) was included in the final wash for 10 min before mounting. For staining of LDs, BODIPY 493/503 (Invitrogen) or LipidTOX (Invitrogen) was included along with the secondary antibodies. Stained cells were analyzed by immunofluorescence microscopy using a Zeiss Axiovert 200M microscope outfitted with a 40× air objective and the appropriate filters. For quantification, immunostained cells were analyzed with equivalent exposure times and the BODIPY 493/503 or LipidTOX fluorescence were inverted for clarity. The size, number, and area of stained LDs were quantified from three independent experiments (average of 500 LDs per experiment) using ImageJ 1.42q, and mean ± SEM was determined. Statistical significance was evaluated using the Student $t$ test with a $P$ value $< 0.05$. The Pearson's correlation coefficient, a measure of colocalization, was determined using the ImageJ Colocalization Finder plugin.

**Cycloheximide Translation Shutoff for Analysis of ATGL Turnover.** To determine the half-life of ATGL, HEK293 cells were incubated in complete growth medium containing the protein translation inhibitor cycloheximide (CHX; 25 μg/mL), and cells were lysed in 1% SDS at 0, 3, 6, and 12 h. SDS-soluble lysates were separated by SDS/PAGE and evaluated by immunoblot analysis with antibodies against ATGL and tubulin. The contribution of proteasomal degradation to ATGL turnover was assessed by adding the proteasome inhibitor MG132 (10 μM) together with CHX. The impact of oleate treatment and the presence of LDs on ATGL half-life was assessed by treating cells with 200 μM oleate

for 12 h before the addition of CHX. Oleate was retained in the medium throughout the course of the experiment.

**Flow Cytometry Analysis of Bimolecular Fluorescence Complementation.** For analysis of bimolecular fluorescence complementation, HEK293 cell lines were transfected with ATGL(S47A)-YFPc, YFPn-CGI-58 or YFPn-UBXD8, and mCherry (also known as Cherry fluorescent protein or ChFP) using FuGENE6 (Roche). The catalytically inactive mutant of ATGL was used to prevent aberrant LD degradation induced by ATGL overexpression. After 5 h of transfection, 200 μM oleate was added, and the cells were shifted to 32 °C for 22 h and then to 30 °C for 2 h to promote maturation of the reconstituted YFP. Cells were then trypsizined, washed in PBS, and analyzed using a BD Biosciences LSRII flow cytometer. Gates were set to enable analysis of mCherry-positive cells, which acted as a coincidence reporter for transfected cells, and the geometric mean of the YFP fluorescence was measured. For comparison of the bimolecular fluorescence complementation in control, UBXD8-S, and UBAC2-S cell lines, YFP fluorescence was normalized by subtraction of YFP fluorescence measured in cells transfected with pcDNA3.1(−), which represents the background YFP fluorescence level. The mean ± SEM was determined from four independent experiments, and statistical significance was assessed using the Student *t* test with $P < 0.05$.

**Measurement of Lipolysis.** HeLa cells expressing empty vector, UBXD8-S, and UBAC2-S were incubated according to the time course shown in Fig. 3*A* (*Lipid Droplet Synthesis and Turnover*). During the 3-h oleate treatment, 0.3 μCi $^{14}$C-oleate (Perkin-Elmer) was included as a radioactive tracer. At the 0 and 3 h time points, cells were washed with PBS, and lipids were extracted with chloroform:methanol (2:1), dried, loaded onto TLC plates, and separated in a solvent of hexane:ethyl ether:acetic acid (80:20:1). Separated lipids were visualized using iodine vapor, TAG was isolated by scraping, and cpm was measured with a Beckman Coulter LS 6500 liquid scintillation counter.


1. Christianson JC, et al. (2012) Defining human ERAD networks through an integrative mapping strategy. *Nat Cell Biol* 14(1):93–105.
2. Christianson JC, Shaler TA, Tyler RE, Kopito RR (2008) OS-9 and GRP94 deliver mutant alpha1-antitrypsin to the Hrd1-SEL1L ubiquitin ligase complex for ERAD. *Nat Cell Biol* 10(3):272–282.
3. Gandotra S, et al. (2011) Human frame shift mutations affecting the carboxyl terminus of perilipin increase lipolysis by failing to sequester the adipose triglyceride lipase (ATGL) coactivator AB-hydrolase-containing 5 (ABHD5). *J Biol Chem* 286(40): 34998–35006.
4. Bence NF, Sampat RM, Kopito RR (2001) Impairment of the ubiquitin-proteasome system by protein aggregation. *Science* 292(5521):1552–1555.
5. DeLaBarre B, Christianson JC, Kopito RR, Brunger AT (2006) Central pore residues mediate the p97/VCP activity required for ERAD. *Mol Cell* 22(4):451–462.


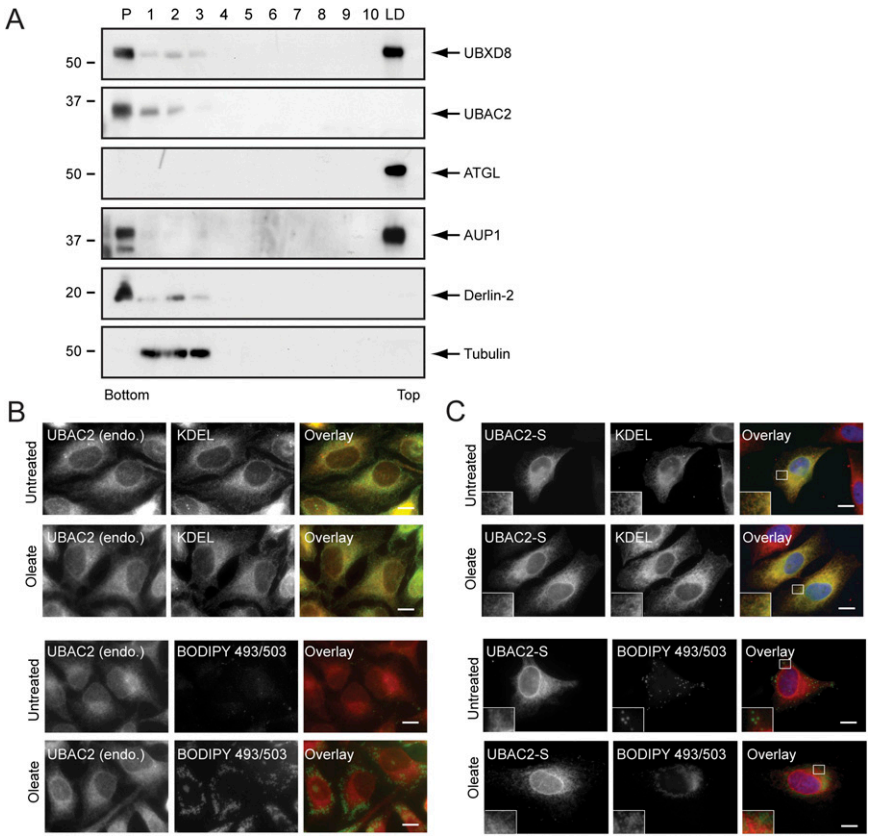


**Fig. S1.** UBAC2 is an endoplasmic reticulum (ER)-resident protein. (*A*) Endogenous UBAC2 is restricted to the ER-enriched pellet (P) fraction while endogenous UBXD8 partitions between ER-enriched and LD-enriched fractions. Biochemical fractionations from HEK293 cells incubated with 200 μM oleate for 16 h were evaluated by immunoblot analysis. Equivalent percentages of each fraction were analyzed. (*B* and *C*) UBAC2 is an ER-resident protein. Immunofluorescence localization of endogenous UBAC2 (anti-UBAC2; red) or UBAC2-S (anti–S-peptide; red), the ER (anti-KDEL; green) or LDs (BODIPY 493/503; green), and nuclei (DAPI; blue) in HeLa cells incubated in the presence or absence of 200 μM oleate for 16 h. White boxes indicate magnified regions. (Scale bars: 10 μm.)

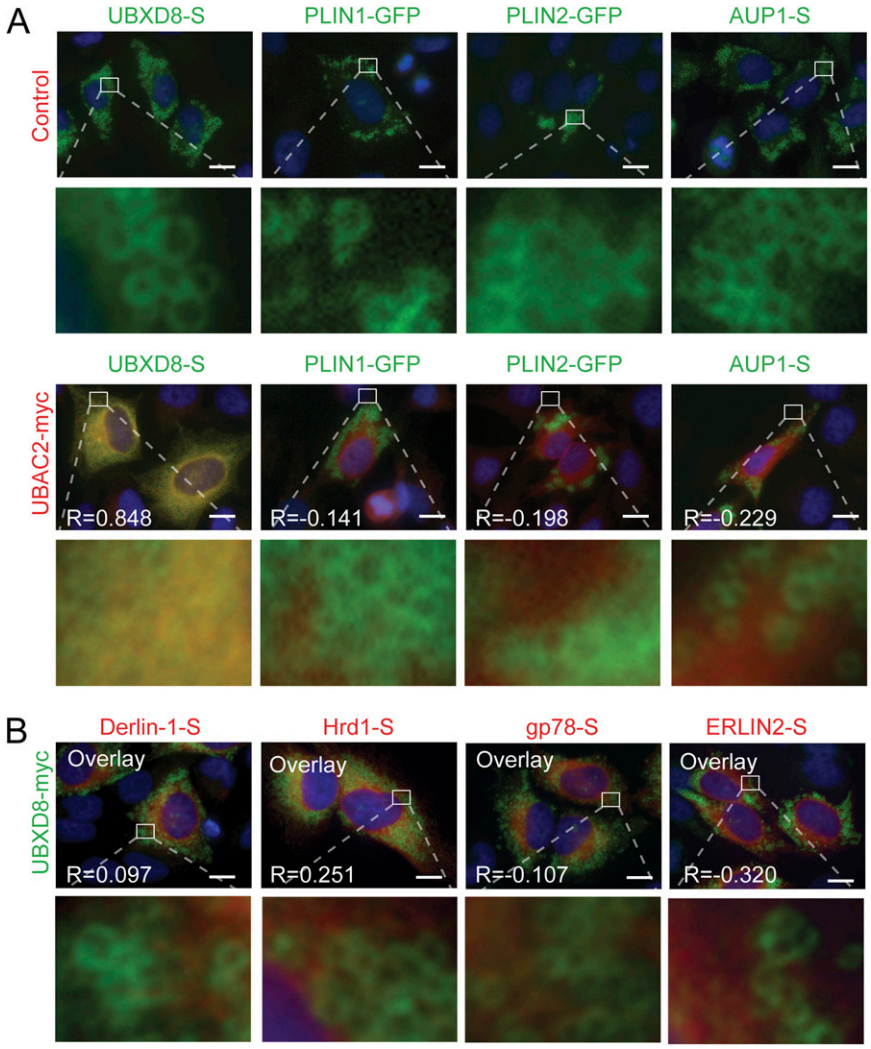


**Fig. S2.** Analysis of the specificity of UBAC2-mediated ER receptor function. (*A*) UBAC2 specifically retains UBXD8 in the ER. The effect of coexpression of UBAC2-myc (anti-myc; red) on the localization of UBXD8-S, AUP1-S, PLIN1-GFP, or PLIN2-GFP (anti–S-peptide or direct fluorescence; green) in HeLa cells treated with 200 μM oleate for 16 h was analyzed by immunofluorescence microscopy. (*B*) UBXD8 trafficking is not restricted by other ER-binding partners. The effect of coexpression of gp78-S, Hrd1-S, Derlin-1-S, or ERLIN2-S (anti–S-peptide; red) on the localization of UBXD8-myc (anti-myc; green) in cells treated with 200 μM oleate for 16 h was analyzed by immunofluorescence microscopy. White boxes indicate magnified regions. Pearson's correlation coefficient is shown in the bottom corner of the micrographs. (Scale bars: 10 μm.)

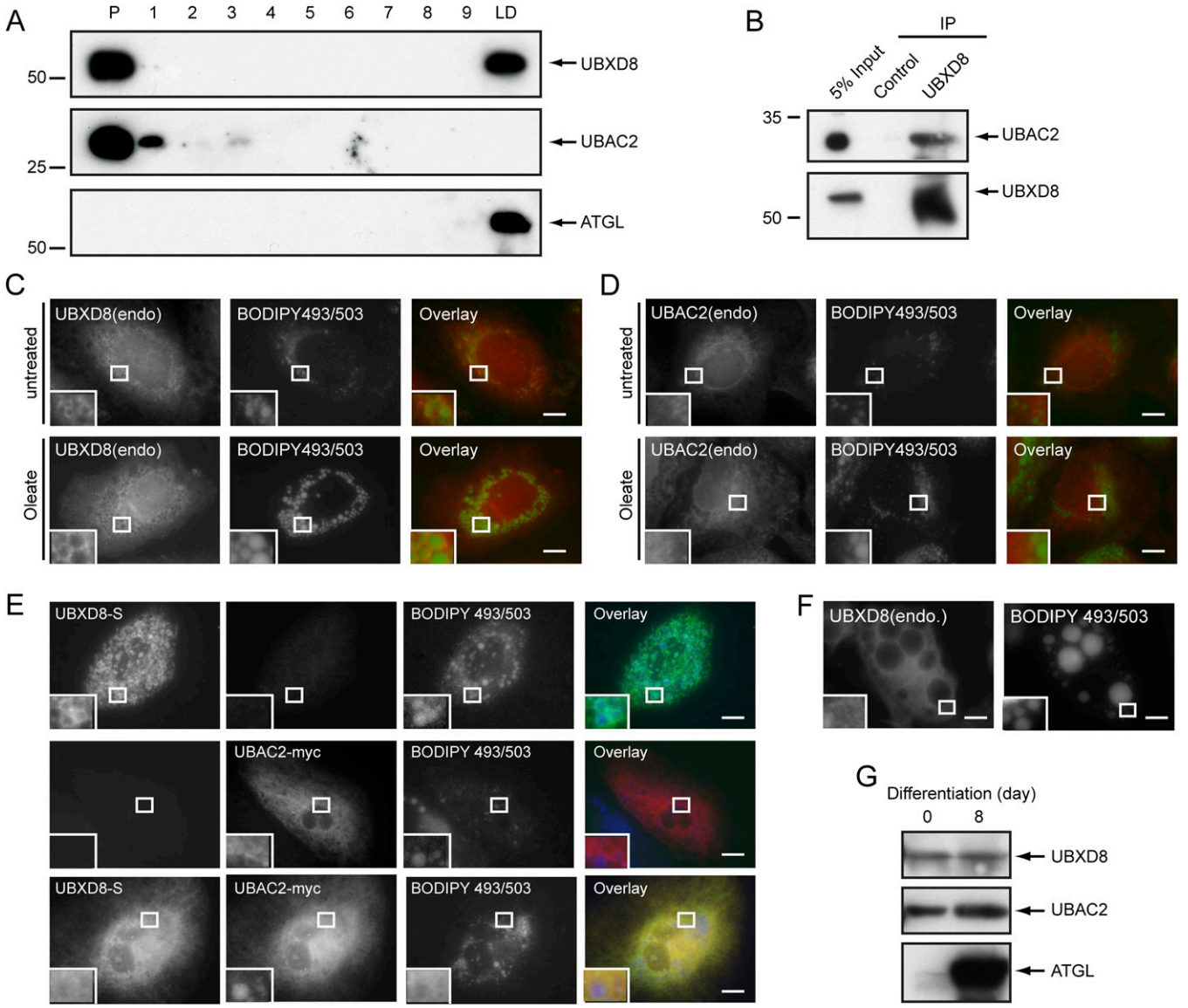


**Fig. S3.** UBAC2 binds and regulates UBXD8 ER-LD partitioning in the Huh7 hepatocyte cell line. (*A*) Endogenous UBXD8 partitions between ER-enriched and LD-enriched fractions in Huh7 cells. Biochemical fractions from Huh7 cells incubated with 200 μM oleate for 24 h were evaluated by immunoblot analysis. (*B*) UBXD8 interacts with UBAC2 in Huh7 cells. Endogenous UBXD8 complexes were immunoprecipitated from Huh7 cells and evaluated by immunoblot analysis. (*C* and *D*) Lipogenic signals induce UBXD8 trafficking to LDs in Huh7 cells. Immunofluorescence localization of endogenous UBXD8 (anti-UBXD8; red) or UBAC2 (anti-UBAC2; red), LDs (BODIPY 493/503; green), and nuclei (DAPI; blue) in Huh7 cells incubated in the presence or absence of 200 μM oleate for 24 h. (*E*) UBAC2 negatively regulates UBXD8 LD trafficking in Huh7 cells. Immunofluorescence localization of UBXD8-S and UBAC2-myc in Huh7 cells cotransfected with a vector control or together. (*F*) UBXD8 is not concentrated on LD membranes in 3T3-L1 adipocytes. Immunolocalization of endogenous UBXD8 in differentiated 3T3-L1 adipocytes. (*G*) UBXD8 is not up-regulated during adipocyte differentiation. SDS-soluble lysates from 3T3-L1 preadipocytes before or after an 8-d differentiation paradigm were analyzed by immunblotting with the indicated antibodies. White boxes indicate magnified regions. (Scale bars: 10 μm.)

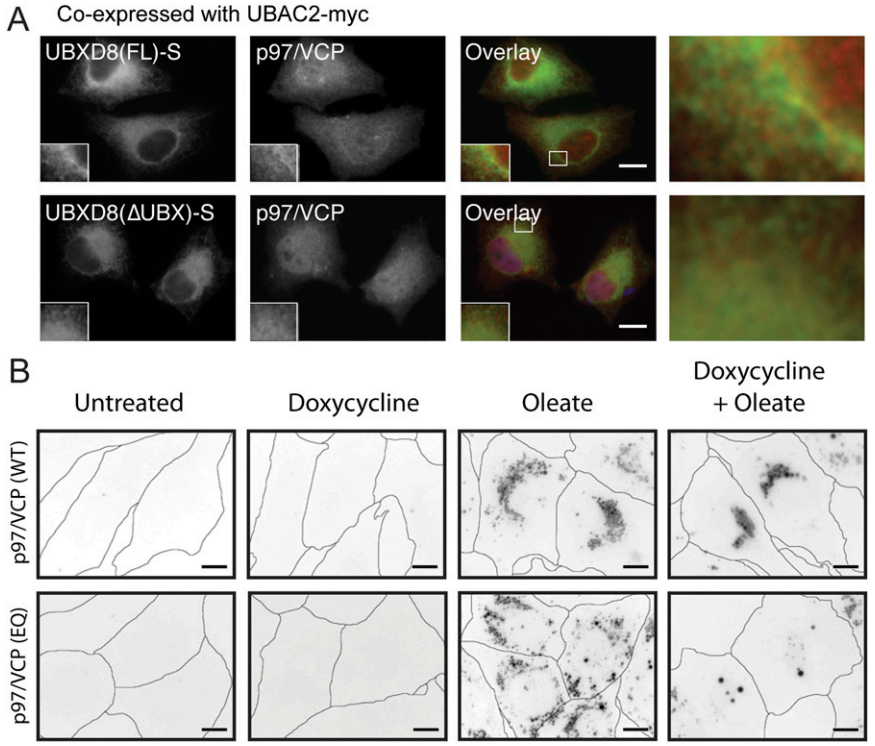


**Fig. S4.** Analysis of UBXD8-dependent p97/VCP LD recruitment and the role of p97/VCP in the regulation of cellular LD stores. (*A*) UBXD8 recruitment of p97/VCP to LDs is blocked by UBAC2 coexpression. The distribution of endogenous p97/VCP (anti-p97/VCP; red) was analyzed in the presence of the indicated UBXD8-S constructs (anti–S-peptide; green) coexpressed with UBAC2-myc in HeLa cells. Nuclei were stained with DAPI (blue). (*B*) p97/VCP ATPase function is required for LD homeostasis. Representative images of U2OS cells expressing inducible p97/VCP(WT) or p97/VCP(EQ) incubated in the presence or absence of 200 μM oleate and doxycycline from the experiment shown in Fig. 2*E*. LDs were stained with BODIPY 493/503 and analyzed by immunofluorescence microscopy. Cells are outlined (black lines) to indicate their boundaries. White boxes indicate magnified regions. (Scale bars: 10 μm.)

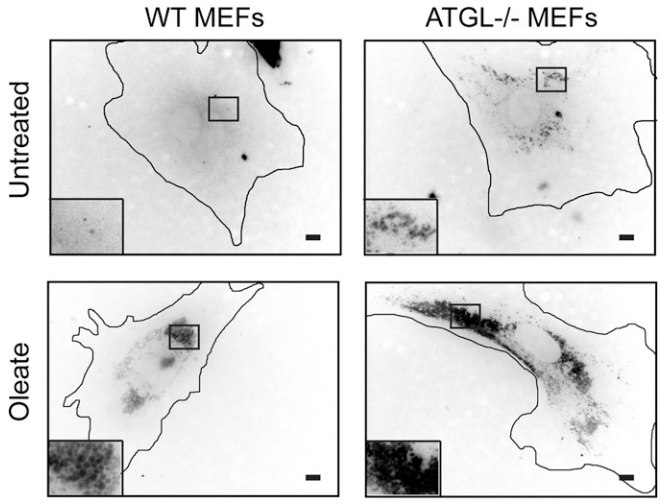


**Fig. S5.** MEFs lacking ATGL retain the ability to induce LD proliferation in response to lipogenic conditions. The LD content in WT and ATGL$^{-/-}$ MEFs was analyzed by staining with BODIPY 493/503 after incubation in the presence and absence of 200 μM oleate for 16 h. The black boxes indicate magnified regions. (Scale bars: 10 μm.)

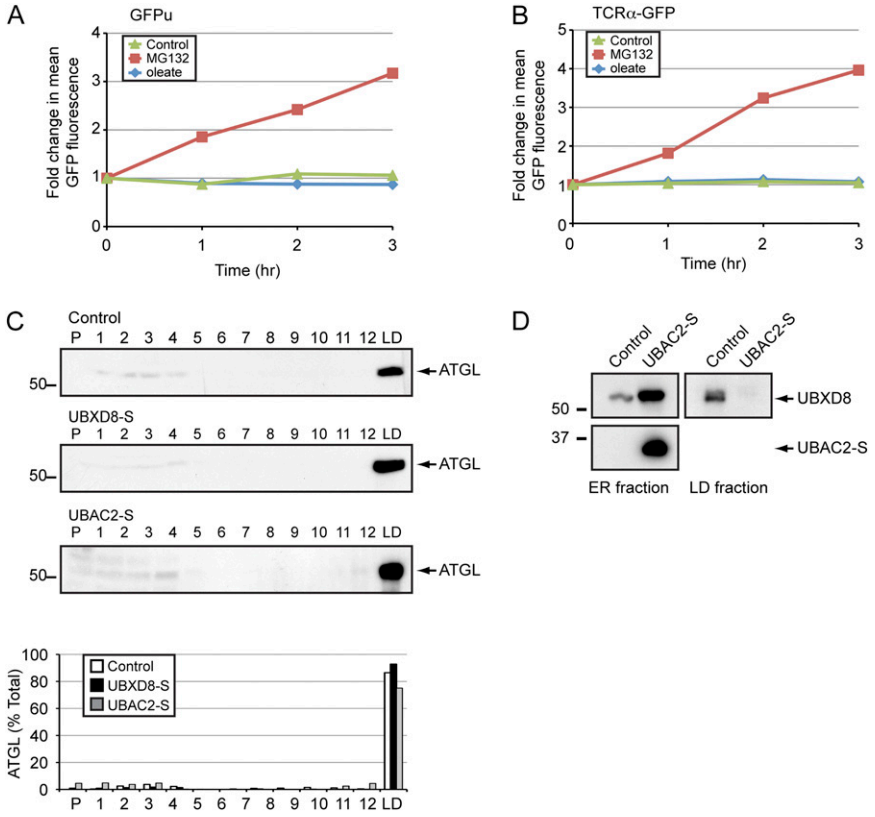


**Fig. S6.** UBAC2 and UBXD8 do not influence the steady-state level or LD association of ATGL. (*A* and *B*) Oleate generally does not inhibit proteasomal degradation. Clonal HEK293 cell lines expressing GFPu or TCRα-GFP were treated as indicated and analyzed by flow cytometry. (*C*) UBXD8 does not influence ATGL LD association. Control HEK293 cells or stable HEK293 cells expressing UBXD8-S or UBAC2-S were incubated with 200 μM oleate for 24 h, fractionated, and evaluated by immunoblot analysis. The relative ATGL levels in each fraction were quantified using ImageJ 1.42q and are presented as a percentage of the total. (*D*) Overexpression of UBAC2 depletes endogenous UBXD8 from LDs. Immunoblot analysis of endogenous UBXD8 in ER- and LD-enriched fractions from oleate-treated control or UBAC2-S–expressing HEK293 cells. Equivalent percentages of each fraction were analyzed.